Muş Alparslan Üniversitesi Fen Bilimleri Dergisi
Muş Alparslan University Journal of Science
ISSN:2147-7930

Cilt/*Volume***:1 Sayı/** *Issue***:1 Haziran/***June***: 2013**

EFFECT OF MOLARITY AND SOLVENT ON THE OPTICAL PARAMETERS OF THE LIQUID-CRYSTALLINE POLYMER F8T2 AND SURFACE MORPHOLOGY PROPERTIES OF THE F8T2 FILM

Bayram GÜNDÜZ*

Muş Alparslan University, Faculty of Education, Department of Science Education, Muş, 49250, Turkey

Abstract

In this study, we investigated the surface morphology of the liquid-crystalline polymer poly[(9,9-dioctylfluorenyl-2,7-diyl)-co-bithiophene] (F8T2) film by high performance atomic force microscopy and the surface roughness parameters of the F8T2 film such as; roughness average (sa), root mean square roughness (sq), surface skewness (ssk) and surface kurtosis (sku) value were obtained. Also, we reported the morphology of the cross-section (wall) and height histogtams of the F8T2 film by AFM. The positive skewness and high kurtosis of the F8T2 film are desirable to achieve low friction applications. The ratios of the sq to the sa for the F8T2 film were found to be 1.271 and 1.292. Then, we investigated in detail the optical properties of the *solutions* of the F8T2 polymer for different molarities and solvents. The absorbance, molar extinction coefficient (ε) and mass extinction coefficient (α) values of the F8T2 polymer decrease with decreasing molarity. The average transmittance, absorption band edge, direct (E_{gd}) and indirect (E_{gid}) energy-gap values of refraction of the F8T2 polymer increase with decreasing molarity. The maximum absorption wavelength (λ_{max}) of the solutions of the F8T2 for 1.200 and 0.800 μM was found to be 455 nm, while the λ_{max} of the F8T2 polymer for DCM, THF and Chloroform solvents were found to be 447, 453 and 455 nm, respectively. The yellow light of the F8T2 polymer is emitted 586 nm. The maximum mass extinction coefficient (α_{max}) values at maximum molar extinction coefficient (ε_{max}) ($2.246x10^6$ and $1.736x10^6$ $Lmol^{-1}cm^{-1}$, respectively) of the solutions of the F8T2 polymer for 1.200 and 0.800 μM were found to be 59.105 and 45.684 $Lg^{-1}cm^{-1}$, respectively, while the α_{max} values at ε_{max} ($2.461x10^6$, $2.371x10^6$ and $2.246x10^6$ $Lmol^{-1}cm^{-1}$, respectively) of the F8T2 polymer for DCM, THF and Chloroform solvents were found to be 64.763, 62.395 and 59.105 $Lg^{-1}cm^{-1}$, respectively. The E_{gd} values (2.413 and 2.387 eV, respectively) of the F8T2 polymer for 0.800 μM and Chloroform solvent are the highest values, while the E_{gd} values (2.220 and 2.279 eV) of the F8T2 polymer for 19.737 μM and THF solvent are the lowest values. The E_{gid} values (2.345 and 2.305 eV, respectively) of the F8T2 polymer for 0.800 μM and Chloroform solvent are the highest values, while the E_{gid} values (2.113 and 2.053 eV) of the F8T2 polymer for 19.737 μM and THF solvent are the lowest values. The obtained E_{gid} values of the F8T2 polymer are more lower than that of the obtained E_{gd} values of the F8T2 polymer. Thus, the optical band-gap of the solution of the F8T2 polymer was decreased with increasing molarity and using THF solvent among DCM, THF and Chloroform solvents.

Keywords: surface roughness parameters, F8T2, molar/mass extinction coefficient, molarity, optical band gap, optical parameters.

Corresponding author: bgunduz83@hotmail.com; b.gunduz@alparslan.edu.tr (B. Gunduz)

Tel.:+904362130013-2104, **Fax:** +904362120853

1. INTRODUCTION

In recent years, organic single crystals grown from small-molecule semiconductors have received increased interest because of their utilization in both fundamental and applied science [1-3]. Polymeric semiconductors (PSs) are a very promising and versatile materials family for flexible electronics [4]. These materials dissolve in common organic solvents and can be processed from a liquid solution [4]. Such solutions are often called 'semiconducting inks' because of the deposition and patterning using low-cost technologies [4]. Conjugated polymers with liquid-crystalline behavior are of great interest for optical and electronic applications [5]. Poly(9,9-dioctylfluorene) (F8), which contains only a fluorene backbone, exhibits blue emission and various morphological behaviors [6-8]. Fluorene-type polymers have emerged as an important class of conducting polymers owing to their efficient emission, high stabilities and relatively high mobility [7]. Fluorene-type polymers also have the potential for full color emission via energy transfer to longer wavelength emitters in blends with other emissive materials [7]. The liquid-crystalline polymer poly[(9,9-dioctylfluorenyl-2,7-diyl)-co-bithiophene] (F8T2) is a promising material for transistor applications as well as optical applications (e.g., solar cells and photodiodes) [5] because it shows high field-effect mobility together with good stability [5,9-11]. The F8T2 polymer exhibits good hole transporting properties [12] and excellent thermotropic liquid crystallinity [13-17]. It has also well been explored in the area of organic field-effect transistors [16], with good hole transporting properties [18].

Atomic Force Microscopy (AFM) image is significant in order to investigate structural properties of a material. AFM has become a popular method of investigating the surface structures of the materials and gives the surface topography images in one dimensional (1D)/three dimensional (3D) by scanning with a cantilever tip over a surface. The knowledge of the surface topography at nanometric resolution made possible to probe dynamic biological process [19,20], tribological properties [21,22], mechanical manufacturing [23] and mainly thin film surfaces [24,25]. It is a useful method to study morphology and texture of diverse surfaces of the materials because of the effect on the electrical and optical properties of the materials/devices [26]. The two key parameters used to characterize the asymmetry and the flatness of the surface distribution are the skewness and kurtosis, which correspond to the third and fourth moments of the density function, respectively [27]. For the Gaussian distribution, the skewness is equal to zero and the kurtosis is equal to three [27].

The nonlinear optical properties, such as optical absorption [28,29], have shown high potential [30] for device applications in far- infrared laser amplifiers [31], photo-detectors [32], and high speed electro-optical modulators [33].

There isn't any reports in the literature about the surface roughness parameters of the only F8T2 polymer film such as; roughness average (sa), root mean square roughness (sq), surface skewness (ssk) and surface kurtosis (sku). Similarly, there isn't any reports about the morphology of the cross-section and height histogtams of the F8T2 polymer

film. There isn't any reports in the literature about the optical properties of the *solutions* of the liquid-crystalline polymer F8T2 for different molarities and solvents. This solution technique for investigation of the optical properties of the soluble materials is more cheaper than a film technique, because I didn't need to any deposition devices such as spin-coater, thermal evaporation devices, which are more expensive devices, to investigate the optical properties of the F8T2 polymer. This solution technique is more accurate than a film technique, because prior, during and after the coating of a film, various impurities may occur on the surface of the film and these disadvantages adversely affect the optical properties of the material.

In this study, we investigated the surface morphology of the liquid-crystalline polymer poly[(9,9-dioctylfluorenyl-2,7-diyl)-co-bithiophene] (F8T2) film by high performance atomic force microscopy and the surface roughness parameters of the F8T2 film such as; roughness average (sa), root mean square roughness (sq), surface skewness (ssk) and surface kurtosis (sku) value were obtained. Also, we are reporting the morphology of the cross-section (wall) and height histogtams of the F8T2 film by AFM. Then, we investigated in detail the optical properties of the *solutions* of the poly[(9,9-dioctylfluorenyl-2,7-diyl)-co-bithiophene] (F8T2) for different molarities and solvents. To investigate optical properties, the F8T2 polymer for different molarities and solvents homogeneously dissolved. The optical measurements were conducted on a Shimadzu model UV-1800 Spectrophotometer. The effect of the molarities and solvents on the optical parameters such as molar extinction coefficient, mass extinction coefficient, average transmittance, absorb wavelength, absorption band edge, direct and indirect optical band gap were investigated. The optical band-gap of the solution of the F8T2 polymer was improved with molarities and solvents.

2. EXPERIMENTAL

The liquid-crystalline polymer poly[(9,9-dioctylfluorenyl-2,7-diyl)-co-bithiophene] (F8T2) and solvents which are Dichloromethane (DCM), Tetrahydrofuran (THF) and Chloroform used in this study were purchased from Sigma–Aldrich Co. The chemical structure of the liquid-crystalline polymer F8T2 is shown in Fig. 1. This section has been occurred in three stages. In the first stage, we prepared the F8T2 film for AFM at 16.447 μM molarity, in the second stage, we prepared the stock solutions of the F8T2 for different molarities and solvents and in the last stage, we recorded optical measurements of the solutions of the F8T2 polymer for different molarities and solvents.

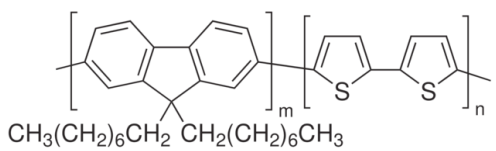

Fig. 1. The chemical structure of the liquid-crystalline polymer F8T2.

2.1. Preparation of the F8T2 film for surface morphology

To prepare the F8T2 film, the F8T2 material weighed with a AND-GR-200 Series Analytical Balance for 16.447 μM, then it was dissolved homogeneously in 10 mL volume of Chloroform and it was filtered through PTFE membrane filter to obtain better film. Ultimately, the solution of the F8T2 filtered was coated on cleaned microscopy glass. After the coating, the film was dried at 80 ºC for 10 minute to evaporate the solvent and remove organic residuals. Surface morphology of the F8T2 film was investigated by high performance atomic force microscopy (hpAFM, NanoMagnetics Instruments Co.) with PPP-XYNCHR type Cantilever at dynamic mode.

2.2. Preparation of the stock solutions of the F8T2 polymer for different molarities and solvents

The average molecular weight and formula of the liquid-crystalline polymer F8T2 is 38000 g/mol [18] and $(C_{37}H_{44}S_2)_n$, respectively. To prepare the stock solutions at different molarities, firstly the F8T2 polymer weighed with a AND-GR-200 Series Analytical Balance for 0.800, 1.200, 2.056, 4.112 and 19.737 μM molarities and for 1.200 μM of the different solvents (DCM, THF and Chloroform). Then, these weighed F8T2 polymers for different molarities (0.800, 1.200, 2.056, 4.112 and 19.737 μM) dissolved homogeneously in 6 mL volume of Chloroform solvent and others which are for different solvents dissolved homogeneously in 6 mL volume of DCM, THF and Chloroform solvents. Finally, prepared all the solutions of the F8T2 polymer were filtered through PTFE membrane filter to obtain better results of the optical measurements. The real pictures of the solutions of the F8T2 polymer dissolved in Chloroform, THF and DCM solvent are shown in Fig. 2.

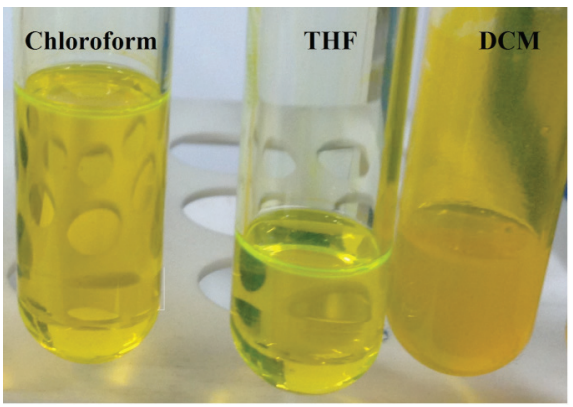

Fig. 2. The real pictures of the solutions of the F8T2 polymer dissolved in Chloroform, THF and DCM solvent.

2.3. The optical measurements of the solutions of the F8T2 polymer for different molarities and solvents

We used the cylindrical cuvettes (Hellma QS-100) of 3.5 mL volume and 10 mm optical path length for all the solutions of the F8T2 polymer. The optical measurements of all the solutions of the F8T2 polymer for different molarities and solvents were recorded by a Shimadzu model UV-1800 Spectrophotometer in the wavelength 1100-190 nm at room temperature.

3. RESULTS AND DISCUSSION

This section has been occurred in three stages. In the first stage, we investigated the surface morphology properties of the F8T2 film. In the second stage, we investigated in detail the optical properties of the solutions of the F8T2 polymer for 0.800, 1.200, 2.056, 4.112 and 19.737 μM. The effect of the molarity on the optical parameters such as molar extinction coefficient, maximum mass extinction coefficient, average transmittance, absorb wavelength, absorption band edge, direct and indirect optical band gap were investigated. In the last stages, we investigated in detail the optical properties of the solutions of the F8T2 polymer for 1.200 μM of the different solvents (DCM, THF and Chloroform). The effect of the DCM, THF and Chloroform solvents on the optical parameters such as molar extinction coefficient, maximum mass extinction coefficient, average transmittance, absorb wavelength, absorption band edge were investigated.

3.1. Surface morphology properties of the F8T2 film

Surface morphology properties of the F8T2 film were investigated by high performance atomic force microscopy. The scan area was chosen as 5x5 μm^2. Figs. 3 show the phase images of the F8T2 film for 5x5 μm^2 scan area, respectively. As seen in Figs. 3, the phase images consist of the bumpy (pit and mound) regions. Similarly, Figs. 4(a,b) show one (1D) and three dimensional (3D) topography images of AFM of the F8T2 film for 5x5 μm^2 scan area, respectively. As seen in Figs. 4(a,b), the topography images also have the light, dark and bumpy regions. The color intensity as seen in Figs. 4(a,b) shows the vertical profile of the material surface, with light regions being the highest points and the dark points representing the depressions and pores [26].

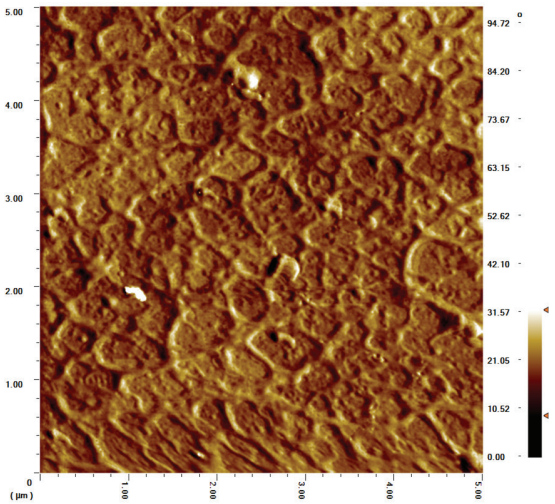

Fig. 3. The phase images of the F8T2 film for 5x5 µm^2 scan area.

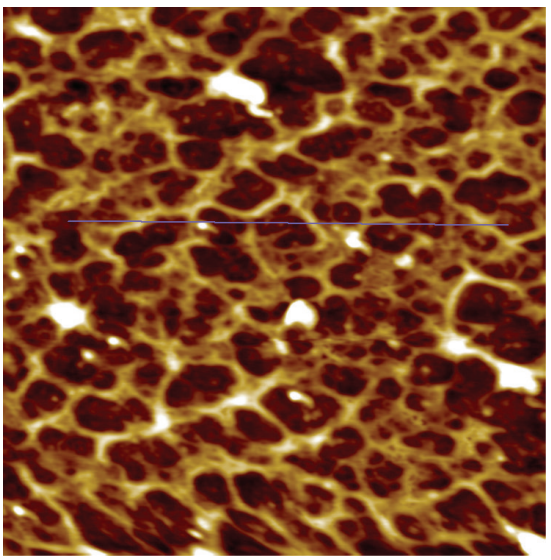

(a)

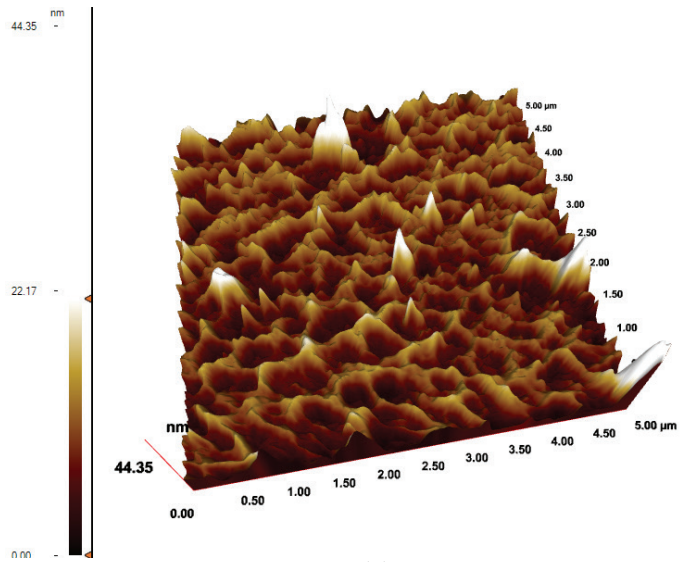

(b)

Fig. 4. (a) One (1D) and **(b)** three dimensional (3D) for 5x5 µm^2 scan area topography images of AFM of the F8T2 film.

The differences in the surface morphology of the F8T2 film investigated in terms of four types of roughness parameters such as; roughness average (*sa*), root mean square roughness (*sq*), surface skewness (*ssk*), and surface kurtosis (*sku*).

In this study, the surface roughness parameters of the F8T2 film such as; roughness average (*sa*), root mean square roughness (*sq*), surface skewness (*ssk*) and surface kurtosis (*sku*) value were obtained from the AFM images with an AFM software program and given in Table 1. As seen in Table 1, the roughness average (sa) values (3.097 and 1.862 nm, respectively) of the F8T2 film for 5x5 µm^2 scan area are lower than that of the root mean square roughness (sq) values (3.936 and 2.406 nm, respectively). For a Gaussian distribution of asperity height, statistical theory shows that the ratio of sq to sa should be 1.25. Ward [34] notes that the asperity height distribution of most engineering surfaces (tribology) may be approximated by a Gaussian distribution with sq/sa values of up to 1.31. The sq/sa values (1.271 and 1.292, respectively) of the F8T2 film for 5x5 µm^2 scan area are reasonably close to the value of 1.25 predicted by theory. This result is significant since it indicates that, at the imaging scale, the asperity height distribution of these surfaces are approximately Gaussian and that the statistical relationships for surface roughness are applicable [20].

As seen in Table 1, the surface skewness (ssk) values (1.230 and 0.713, respectively) of the F8T2 film for 5x5 µm^2 scan area are positive values which positive values show that the peaks are dominant on the surface. The distribution of positive and negative values indicates the existence of protruding grains [20] and presence of peaks is prevailing [35].

Surfaces with a positive skewness, such as turned surfaces have fairly high spikes that protrude above a flatter average [26]. Skewness describes the asymmetry of the height distribution (HD) and is equal to 0 for a Gaussian surface [36]. The surface of the F8T2 film for 5x5 μm^2 scan area have a simple shape and more advanced parameters are needed to fully describe the surface structure because of the ssk values (1.230 and 0.713) <1.5. It is observed that positive skewness values of the F8T2 film predict higher contact force, real area of contact, number of contacting asperities, tangential and adhesion forces than the Gaussian case [27]. It is observed that positive skewness of the F8T2 film results in lower friction coefficient values than the Gaussian case [27]. A positive ssk values of the F8T2 film as seen also in Figs. 4(a,b) indicate a surface with islands and an asymmetry in the height histogram and an additional Gaussian component in the HD [36].

Kurtosis is a measure of the sharpness of the surface height distribution and for a Gaussian surface equals 3 [36]. As seen in Table 1, the surface kurtosis (sku) values (7.836 and 4.192, respectively) of the F8T2 film for 5x5 μm^2 scan area are higher than 3 which indicate the low valleys with bumpy surface as seen also in Figs. 4(a,b). In the literature [30], for spiky surfaces, sku>3; for bumpy surfaces, sku<3; perfectly random surfaces have kurtosis 3. The results of the sku values of the F8T2 film show that the F8T2 film indicates spiky [20] and sharp islands or holes [36] surfaces as seen in Figs. 4(a,b). It is known that the rough surfaces with positive skewness and high kurtosis values reduce friction [37,38]. The positive skewness and high kurtosis of the F8T2 film are desirable to achieve low friction applications [27]. The distributions with kurtosis values higher than three of the F8T2 film predict higher contact and friction parameters with larger deviations compared to the Gaussian case [27]. The effect of skewness and kurtosis on the static friction coefficient is significant practical engineering field [27]. The effect of kurtosis on the static friction coefficient of the F8T2 film is different, because different trends are observed for kurtosis >3 [27].

Figs. 5(a,b) show the histogram and cross-section plots of the F8T2 film for 5x5 μm^2 scan area, respectively. The histogram is a graph of neighboring columns (or bins). Each column represents a height range. The height of each column represents the number of image pixels which have a height value in the particular range. As seen in Fig. 5a, all columns have the same width, i.e. they represent the same height span. If the surface is random, the histogram will be bell shaped with the bell top at the mean height in the image [39].

Table 1. The roughness average (sa), root mean square roughness (sq), surface skewness (ssk) and surface kurtosis (sku) values of the F8T2 film.

5x5 μm^2 scan area				**1x1 μm^2 scan area**			
sa (nm)	***sq (nm)***	**ssk**	**sku**	**sa (nm)**	***sq (nm)***	**ssk**	**sku**
3.097	3.936	1.230	7.836	1.862	2.406	0.713	4.192

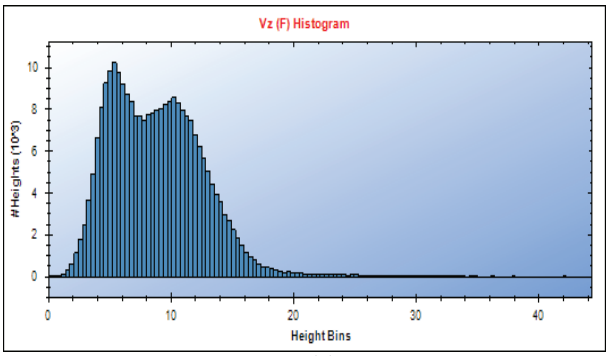

(a)

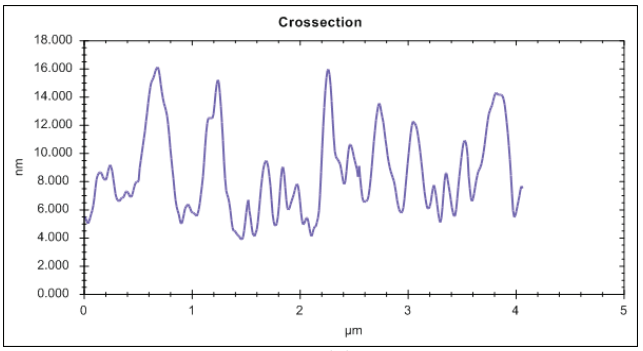

(b)

Fig. 5. (a) The histogram and **(b)** cross-section for 5x5 µm^2 scan area plots of the F8T2 film.

3.2. The effect on optical parameters of the molarity

The absorbance (Abs.) spectra of the solutions of the F8T2 were taken to investigate their optical properties for 0.800, 1.200, 2.056, 4.112 and 19.737 µM molarities and the plot of the absorbance vs. wavelength is shown in Fig. 6. As seen in Fig. 6, the absorbance values of the solutions of the F8T2 exist in the near ultraviolet (200-380 nm) and visible region (380-780 nm). This shows that the near ultraviolet and visible regions are very significant regions for the liquid-crystalline polymer F8T2. As seen in Fig. 6, the uncertainty which results from the high molarity in the absorbance values of the solution of the F8T2 for 19.737, 4.112 and 2.056 µM molarities in the range of about 250 and 510 nm is becoming gradually disappear with decreasing molarity and all the absorbance values of the F8T2 can be clearly appeared after the molarity values of less than 2.056 µM. As seen in Fig. 6, the absorbance values of the F8T2 polymer decrease with decreasing molarity and there is a pit in the near ultraviolet and there is a peak in the visible region. The maximum absorption wavelength (λ_{max}) of the solutions

of the F8T2 for 1.200 and 0.800 µM was found to be 455 nm. It is observed that the Abs_{max} value of the solution of the F8T2 was obtained in the visible region. Thus, the absorbance (Abs_{max}) values at λ_{max} of the solutions of the F8T2 polymer for 1.200 and 0.800 µM were found to be 2.695 and 1.389, respectively. It is observed that the Abs_{max} value of the solution of the F8T2 polymer can be decreased with decreasing molarity. As seen in Fig. 6, the curves of the plots of the solutions of the F8T2 polymer in the near ultraviolet region consist of the maximum and minimum absorption wavelengths. The maximum absorption wavelengths (λ_{max}) of the solutions of the F8T2 for 4.112, 2.056, 1.200 and 0.800 µM were found to be about 250 nm. The minimum absorption wavelengths (λ_{min}) of the solutions of the F8T2 for 4.112, 2.056, 1.200 and 0.800 µM were found to be about 312 nm. It is observed that the pits of the solutions of the F8T2 were obtained in the near ultraviolet region. Finally, as seen in Fig. 6, the absorbance values of the solutions of the F8T2 polymer sharply decrease after λ_{max} value (at 455 nm) and the yellow light of the F8T2 polymer is emitted 586 nm. This situation is very significant and is prefered for high spectral optical/electrical/opto-electronic devices.

The molar extinction coefficient (ε) values of the solutions of the F8T2 polymer can be determined with an equation known as the Beer–Lambert law [40],

$$\varepsilon = \frac{Abs}{\mathit{l}c} \qquad (1)$$

where Abs is an actual absorption, l is an optical path length, and c is the molar concentration of the used cuvettes. The ε values of the solutions of the F8T2 were calculated from Eq. (1). The ε plot of the solutions of the F8T2 polymer for 0.800, 1.200, 2.056, 4.112 and 19.737 µM is shown in Fig. 7. As seen in Fig. 7, the ε values of the solutions of the F8T2 polymer exist in the near ultraviolet and visible region. As seen in Fig. 7, the ε values of the F8T2 polymer can be clearly appeared after the molarity values of less than 2.056 µM.

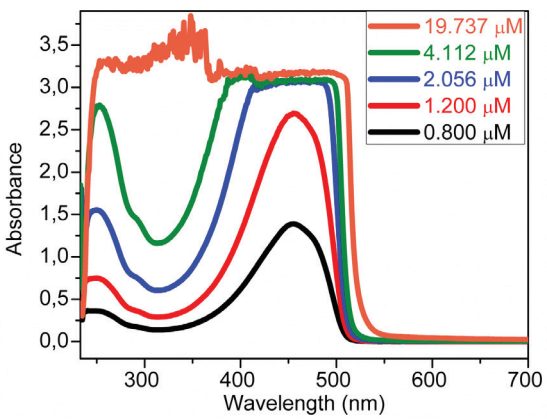

Fig. 6. The plot of the absorbance vs. wavelength of the solutions of the F8T2 polymer for 0.800, 1.200, 2.056, 4.112 and 19.737 µM.

As seen in Fig. 7, the molar extinction coefficient of the F8T2 polymer decreases with decreasing molarity. The maximum molar extinction coefficient (ε_{max}) at λ_{max} value (455 nm) of the solutions of the F8T2 polymer for 1.200 and 0.800 µM were found to be $2.246x10^6$ and $1.736x10^6$ $Lmol^{-1}cm^{-1}$, respectively. It is observed that the ε_{max} value of the solution of the F8T2 polymer can be decreased with decreasing molarity. The ε values of the solutions of the F8T2 polymer sharply decrease after λ_{max} value (at 455 nm). It is observed that the molar extinction coefficient values of the F8T2 polymer are the lowest values for yellow light emitted at 586 nm.

The mass extinction coefficients (α) can be calculated by [41],

$$\alpha = \frac{\varepsilon}{M_A} \tag{2}$$

where M_A is the molecular mass of the material which is the average 38000 g/mol [18] of the liquid-crystalline polymer F8T2. The maximum mass extinction coefficient (α_{max}) at ε_{max} values ($2.246x10^6$ and $1.736x10^6$ $Lmol^{-1}cm^{-1}$, respectively) of the solutions of the F8T2 polymer for 1.200 and 0.800 µM were found to be 59.105 and 45.684 $Lg^{-1}cm^{-1}$, respectively. It is observed that the α_{max} value of the solution of the F8T2 polymer can be decreased with decreasing molarity.

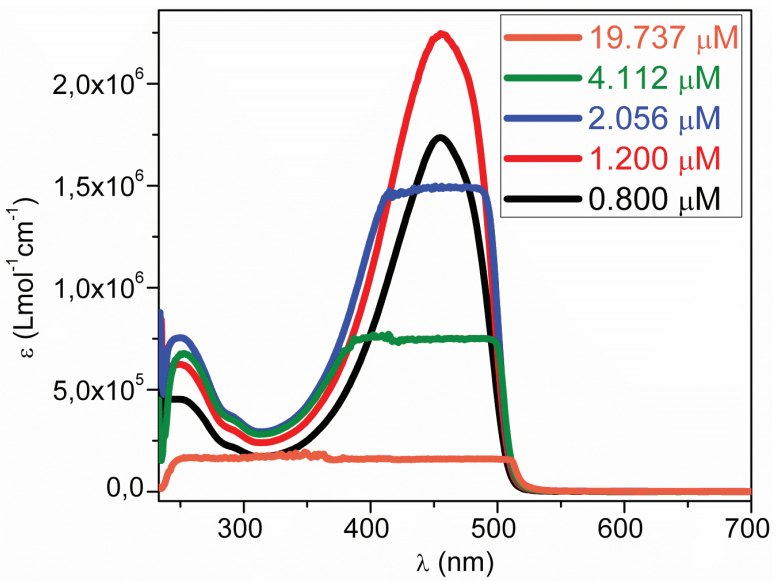

Fig. 7**.** The molar extinction coefficient (ε) plot vs. λ of the solutions of the F8T2 polymer for 0.800, 1.200, 2.056, 4.112 and 19.737 µM.

The transmittance spectra of the solutions of the F8T2 polymer were taken to investigate their optical properties for 0.800, 1.200, 2.056, 4.112 and 19.737 µM and

the plot of the transmittance vs. wavelength is shown in Fig. 8a. As seen in Fig. 8a, the transmittance spectra of the solutions of the F8T2 polymer exists in the near ultraviolet and visible region and the transmittance of the F8T2 polymer increases with decreasing molarity. As seen in Fig. 8a, the uncertainty which results from the high molarity in the transmittance spectra of the solution of the F8T2 polymer for 19.737, 4.112 and 2.056 μM in the range of about 250 and 510 nm is becoming gradually disappear with decreasing molarity and all the transmittance values of the F8T2 polymer can be clearly appeared after the molarity values of less than 2.056 μM. As seen in Fig. 8a, there is a peak in the near ultraviolet and there is a pit for 0.800 μM in the visible region and the transmittance spectra of the solutions of the F8T2 polymer for 0.800 μM sharply increases in the range of about 455 and 525 nm. In the near ultraviolet and visible region, the average transmittance (T_{avg}) values of the solutions of the F8T2 polymer for 0.800, 1.200, 2.056, 4.112 and 19.737 μM were calculated and given in Table 2. As seen in Table 2, the T_{avg} values of the F8T2 polymer in the visible region are higher than that of the values in the near ultraviolet region. As seen in Table 2, the T_{avg} values (59.162 and 73.160%, respectively) of the F8T2 polymer for 0.800 μM in the near ultraviolet and visible region are the highest values, while the T_{avg} values (0.992 and 57.852%, respectively) for 19.737 μM are the lowest values. It is observed that the average transmittance values of the solutions of the F8T2 in the near ultraviolet and visible region decrease with increasing molarity. To estimate the absorption band edge of the solutions of the F8T2 polymer, the first derivative of the optical transmittance can be computed. For this purpose, we plotted the curves of $dT/d\lambda$ versus λ of the solutions of the F8T2 polymer for 0.800, 1.200, 2.056, 4.112 and 19.737 μM, as shown in Fig. 8b. As seen in Fig. 8b, the maximum peak position corresponds to the absorption band edge and there is a small shift in the direction of the higher wavelengths with increasing molarity. The absorption band edge values of the solutions of the F8T2 for 0.800, 1.200, 2.056, 4.112 and 19.737 μM were calculated from the maximum peak position and given in Table 2. As seen in Table 2, the maximum peak values of the solutions of the F8T2 polymer vary from 523 to 563 nm. This result suggests that the absorption band edge values of the solutions of the F8T2 polymer shift from 2.371 to 2.203 eV with increasing molarity, that is, the absorption band edge of the solutions of the F8T2 polymer decreases with increasing molarity.

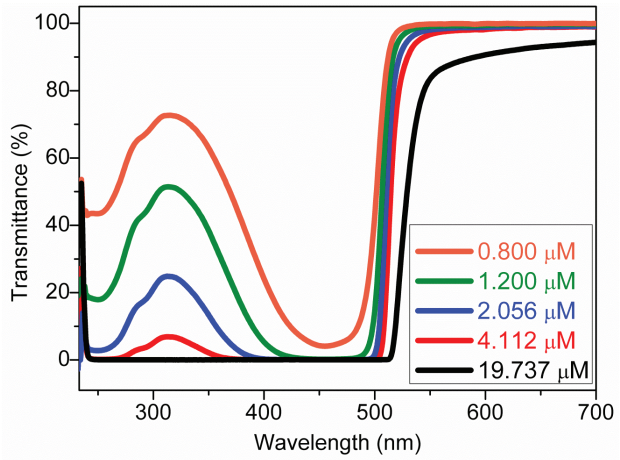

(a)

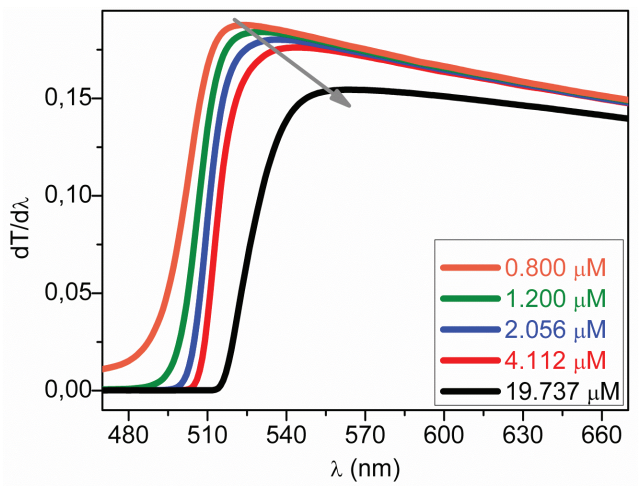

(b)

Fig. 8. (a) The plot of the transmittance vs. λ and **(b)** the curves of dT/dλ vs. λ of the solutions of the F8T2 polymer for 0.800, 1.200, 2.056, 4.112 and 19.737 μM.

The optical band gap of optical transitions can be obtained dependence of absorption coefficient (α) on photon energy. It is evaluated that the band structure of the solution obeys the rule of direct transition and in a direct band gap material; the absorption coefficient dependence on photon energy is analyzed by [42],

$$\alpha = A(h\nu - E_g)^m \qquad (3)$$

where A is a constant, hν is the photon energy, E_g is the optical band and m is the parameter measuring type of band gaps. To determine the optical band gap of the solutions of the F8T2 polymer for 0.800, 1.200, 2.056, 4.112 and 19.737 μM, the $(\alpha h\nu)^2$ plot vs.

the photon energy E of the F8T2 polymer is shown in Fig. 9a. As seen in Fig. 9a, there is a linear region for the direct band gap E_{gd} values of the F8T2 polymer. By extrapolating the linear plot to $(\alpha h\nu)^2=0$, the E_{gd} values of the F8T2 polymer were obtained and given in Table 2. As seen in Table 2, the E_{gd} value (2.413 eV) of the F8T2 polymer for 0.800 µM is the highest value of all the molarities, while the E_{gd} value (2.220 eV) of the F8T2 polymer for 19.737 µM is the lowest value. This suggests that the direct energy-gap of the F8T2 polymer can be more decreased with increasing molarity. Similarly, the dependence on photon energy E of $(\alpha h\nu)^{1/2}$ for indirect band gap region of the solutions of the F8T2 polymer for 0.800, 1.200, 2.056, 4.112 and 19.737 µM is shown in 9b. As seen in Fig. 9b, there is a linear region for the indirect band gap of the F8T2 polymer. By extrapolating the linear plot to $(\alpha h\nu)^{1/2}=0$ at the linear region, the indirect energy gap E_{gid} values of the F8T2 polymer were obtained and given in Table 2. The E_{gid} value (2.345 eV) of the F8T2 polymer for 0.800 µM is the highest value of all the molarities, while the E_{gid} value (2.113 eV) of the F8T2 for 19.737 µM is the lowest value. The E_{gd} and E_{gid} values of the F8T2 polymer were in agreement with the 2.4 eV [7,16] and 2.28 eV [43] values in the literature. This small discrepancy in the band-gap of the F8T2 polymer originates from difference of the molarity, process of the coating of the film and calculating method of the optical band-gap. This results suggest that the indirectc energy-gap of the F8T2 polymer can be more decreased with increasing molarity. It is observed that the obtained optical indirect energy-gap E_{gid} values of the F8T2 polymer are more lower than that of the obtained optical direct energy-gap E_{gd} values of the F8T2 polymer. As seen in Table 2, the obtained E_{gd} and E_{gid} values from the plots of $(\alpha h\nu)^2$ and $(\alpha h\nu)^{1/2}$ vs. E of the F8T2 polymer for 0.800, 1.200, 2.056, 4.112 and 19.737 µM are close to values of the first decrease of transmittance of the F8T2 polymer anda re close to values of the absorption band edge of the F8T2 polymer. It is observed that the optical band-gap of the F8T2 polymer can be found from the plots of $(\alpha h\nu)^2$ and $(\alpha h\nu)^{1/2}$ vs. E, the absorption band edge and the first decrease of transmittance spectra of the F8T2 polymer.

Table 2. The $T_{avg\text{-}NU}$ (in the near ultraviolet region), $T_{avg\text{-}V}$ (in the visible region), $\lambda_{max.\ peak}$, absorption band edge, $E_{gd,}$ $E_{gid,}$ λ_{Tfd} (wavelengths at first decrease of transmittance) and E_{Tfd} values of the solutions of the F8T2 for 0.800, 1.200, 2.056, 4.112 and 19.737 µM.

Molarity (µM)	**$T_{avg\text{-}NU}$ (%)**	**$T_{avg\text{-}V}$ (%)**	**$\lambda_{max.\ peak}$ (nm)**	**Absorption band edge (eV)**	**E_{gd} (eV)**	**E_{gid} (eV)**	**λ_{Tfd} (nm)**	**E_{Tfd} (eV)**
0.800	59.162	73.160	523	2.371	2.413	2.345	522	2.376
1.200	35.038	68.576	531	2.335	2.387	2.305	528	2.349
2.056	12.845	66.333	536	2.313	2.361	2.265	534	2.322

4.112	3.131	64.934	545	2.275	2.333	2.225	545	2.275
19.737	0.992	57.852	563	2.203	2.220	2.113	561	2.210

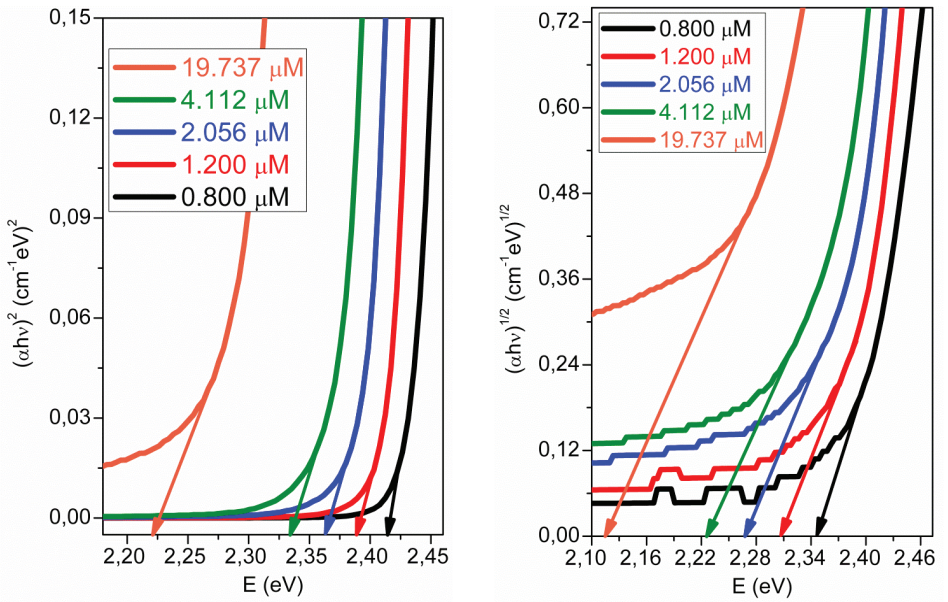

Fig. 9. (a) The $(\alpha h\nu)^2$ plot vs. the photon energy (E) **(b)** the $(\alpha h\nu)^{1/2}$ plot vs. E of the F8T2 polymer for 0.800, 1.200, 2.056, 4.112 and 19.737 μM.

3.3. The effect on optical parameters of the solvents

The Abs. spectra of the solutions of the F8T2 polymer were taken to investigate their optical properties for 1.200 μM of the DCM, THF and Chloroform solvents and the plot of the Abs. vs. λ is shown in Fig. 10. As seen in Fig. 10, the absorbance values of the solutions of the F8T2 polymer exist in the near ultraviolet and visible region. Although there is a small difference absorbance of the F8T2 polymer for DCM, THF and Chloroform solvents, the curves of the absorbance of the F8T2 polymer are compatible with each other. The maximum absorption wavelengths (λ_{max}) of the solutions of the F8T2 polymer for DCM, THF and Chloroform solvents were found to be 447, 453 and 455 nm, respectively. It is observed that the Abs_{max} values of the solution of the F8T2 polymer were obtained in the visible region. Thus, the Abs_{max} values at λ_{max} of the solutions of the F8T2 polymer for DCM, THF and Chloroform solvents were found to

be 2.953, 2.845 and 2.695, respectively. It is observed that the Abs_{max} value (2.953) of the solution of the F8T2 polymer for DCM solvent is the highest value, while the Abs_{max} value (2.695) of the F8T2 polymer for Chloroform solvent is the lowest value. Finally, as seen in Fig. 10, the absorbance values of the solutions of the F8T2 polymer sharply increase until λ_{max} values of the F8T2 polymer, then the absorbance values sharply decrease after these λ_{max} values.

The molar extinction coefficient (ε) values of the solutions of the F8T2 polymer for DCM, THF and Chloroform solvents were calculated from Eq. (1). The ε plot vs. λ of the F8T2 polymer is shown in Fig. 11. The maximum molar extinction coefficient (ε_{max}) values at λ_{max} (at 447, 453 and 455 nm, respectively) of the F8T2 polymer for DCM, THF and Chloroform solvents were found to be $2.461x10^6$, $2.371x10^6$ and $2.246x10^6$ $Lmol^{-1}cm^{-1}$, respectively. It is observed that the ε_{max} value ($2.246x10^6$ $Lmol^{-1}cm^{-1}$) of the F8T2 polymer for Chloroform solvent is the lowest value, while the ε_{max} value $2.461x10^6$ $Lmol^{-1}cm^{-1}$) of the F8T2 polymer for DCM solvent is the highest value.

The maximum mass extinction coefficient (α_{max}) at ε_{max} values $2.461x10^6$, $2.371x10^6$ and $2.246x10^6$ $Lmol^{-1}cm^{-1}$, respectively) of the F8T2 polymer for DCM, THF and Chloroform solvents were calculated from Eq. (2) and found to be 64.763, 62.395 and 59.105 $Lg^{-1}cm^{-1}$, respectively. It is observed that the α_{max} value (64.763 $Lg^{-1}cm^{-1}$) of the F8T2 polymer for DCM solvent is the highest value, while the α_{max} value (59.105 $Lg^{-1}cm^{-1}$) of the F8T2 polymer for Chloroform is the lowest value. It is observed that the α_{max} value of the solution of the F8T2 polymer can be changed with different solvents.

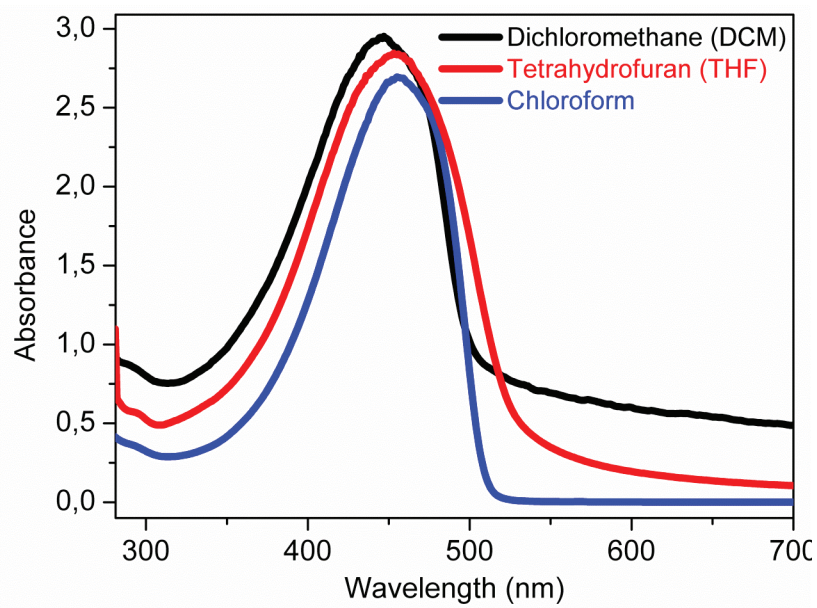

Fig. 10. The plot of the absorbance vs. wavelength of the solutions of the F8T2 polymer for 1.200 μM of the DCM, THF and Chloroform solvents.

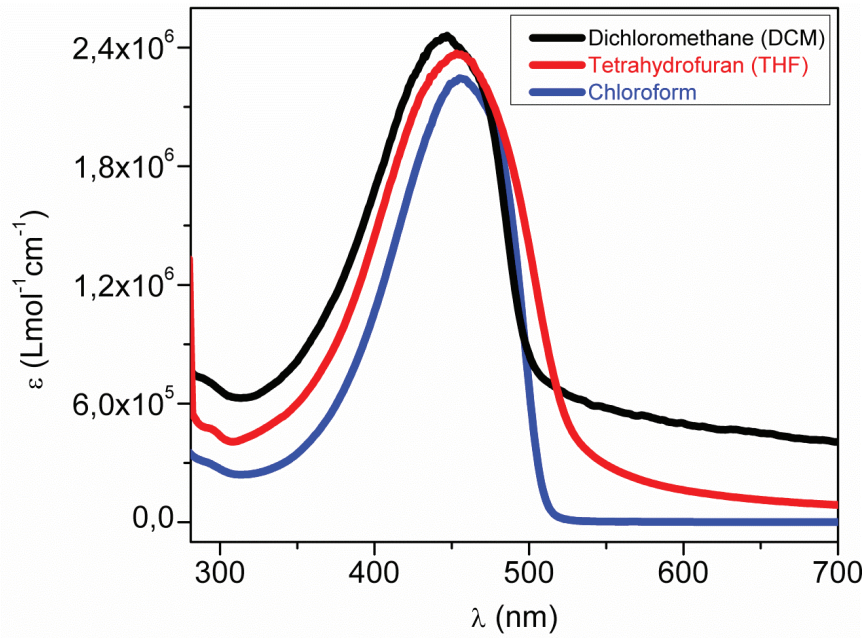

Fig. 11. The molar extinction coefficient (ε) plot vs. λ of the solutions of the F8T2 polymer for DCM, THF and Chloroform solvents.

The plot of the transmittance vs. λ of the F8T2 polymer for DCM, THF and Chloroform solvents is shown in Fig. 12a. As seen in Fig. 12a, there is a peak in the near ultraviolet and there is a pit in the visible region. In the near ultraviolet and visible region, the average transmittance (T_{avg}) values of the solutions of the F8T2 polymer for DCM, THF and Chloroform solvents were calculated and given in Table 3. As seen in Table 3, the T_{avg} values of the F8T2 polymer in the visible region are higher than that of the values in the near ultraviolet region. As seen in Table 3, the T_{avg} values (11.302 and 19.150%, respectively) of the F8T2 polymer for DCM in the near ultraviolet and visible region are the lowest values, while the T_{avg} values (35.038 and 68.576%, respectively) for Chloroform solvent are the highest values. These results show that the solvents are significant effect on the transmittance values of the F8T2 polymer in the near ultraviolet and visible region. To estimate the absorption band edge of the F8T2 polymer, we plotted the curves of dT/dλ vs. λ of the F8T2 polymer for DCM, THF and Chloroform solvents, as shown in Fig. 12b. As seen in Fig. 12b, there is a big shift in the curves of dT/dλ of the F8T2 with different solvents and is an uncertainty in the curves of dT/dλ of the F8T2 for DCM and THF solvents, but the maximum peak can be clearly appeared for Chloroform. Thus, we can calculate the absorption band edge value (2.335 eV) of the F8T2 polymer for Chloroform, but the absorption band edge values of the F8T2 polymer for DCM and THF solvents can not be accurately calculat ed from the maximum peak position.

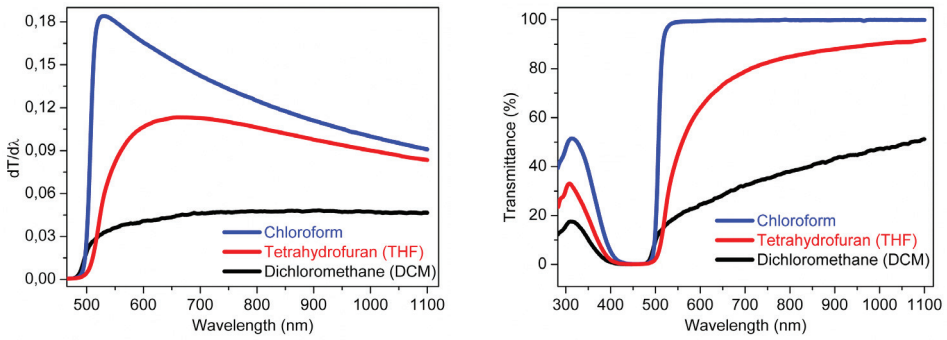

Fig. 12. (a) The plot of the transmittance vs. λ and **(b)** the curves of dT/dλ vs. λ of the solutions of the F8T2 polymer for DCM, THF and Chloroform solvents.

To determine the optical band gap E_g of the solutions of the F8T2 polymer for DCM, THF and Chloroform solvents, the $(\alpha h\nu)^2$ plot vs. the photon energy E of the F8T2 polymer is shown in Fig. 13a. The E_{gd} values of the F8T2 polymer were obtained and given in Table 3. As seen in Table 3, the E_{gd} value (2.387 eV) of the F8T2 polymer for Chloroform solvent is the highest value, while the E_{gd} value (2.279 eV) of the F8T2 polymer for THF solvent is the lowest value. This suggests that the direct energy-gap of the F8T2 polymer changes with different solvents. Similarly, the dependence on photon energy E of $(\alpha h\nu)^{1/2}$ for indirect band gap E_{gid} region of the solutions of the F8T2 polymer for DCM, THF and Chloroform solvents is shown in 13b. The E_{gid} values of the F8T2 polymer were obtained and given in Table 3. As seen in Table, the E_{gid} value (2.305 eV) of the F8T2 polymer for Chloroform solvent is the highest value, while the E_{gid} value (2.053 eV) of the F8T2 polymer for THF solvent is the lowest value. The E_{gd} and E_{gid} values of the F8T2 polymer were in agreement with the 2.4 eV [7,16] and 2.28 eV [43] values in the literature. These results suggest that the E_{gd} and E_{gid} values for THF solvent are lower than that of the values for Chloroform solvent and the obtained E_{gid} values of the F8T2 are more lower than that of the obtained E_{gd} values of the F8T2 polymer. Thus, to obtain more lower direct and/or indirect energy-gap of the F8T2 polymer can be prefered THF solvent.

Table 3. The $T_{avg\text{-}NU}$ (in the near ultraviolet region), $T_{avg\text{-}V}$ (in the visible region), E_{gd} and $E_{gid,}$ values of the solutions of the F8T2 for DCM, THF and Chloroform solvents.

Solvents	$T_{avg\text{-}NU}$ (%)	$T_{avg\text{-}V}$ (%)	E_{gd} (eV)	E_{gid} (eV)
DCM	11.302	19.150	2.308	2.153
THF	20.019	44.796	2.279	2.053
Chloroform	35.038	68.576	2.387	2.305

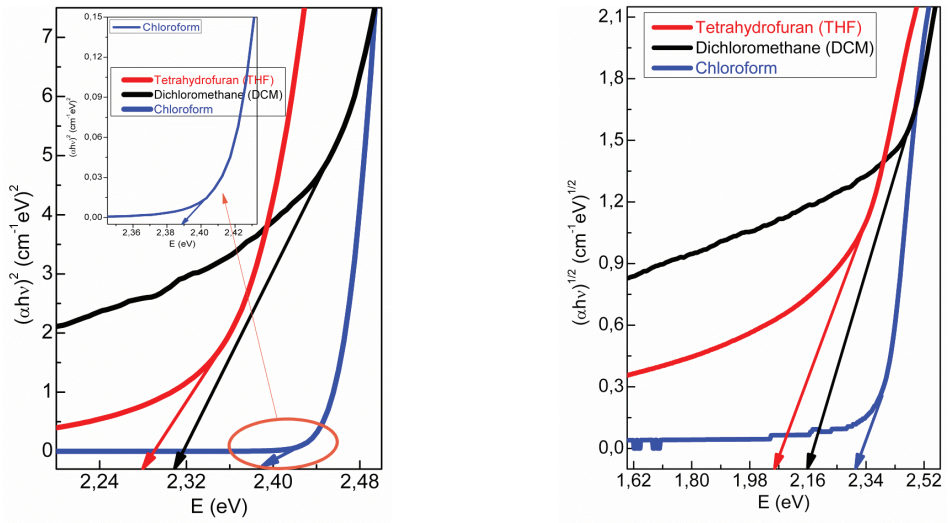

Fig. 13. (a) The $(\alpha h\nu)^2$ plot vs. the photon energy (E) **(b)** the $(\alpha h\nu)^{1/2}$ plot vs. E of the F8T2 polymer for DCM, THF and Chloroform solvents.

4. CONCLUSIONS

We investigated the surface morphology of the liquid-crystalline polymer F8T2 film by high performance atomic force microscopy and reported the morphology of the cross-section (wall) and height histogtams of the F8T2 film by AFM. The positive skewness and high kurtosis of the F8T2 film are desirable to achieve low friction applications. The root mean square roughness (sq)/the roughness average (sa) values (1.271 and 1.292, respectively) of the F8T2 film for 5x5 μm^2 and 1x1 μm^2 scan area are reasonably close to the value of 1.25 predicted by theory. Then, we investigated in detail the optical properties of the *solutions* of the F8T2 polymer for different molarities and solvents. This solution technique for investigation of the optical properties of the soluble materials is more cheaper than a film technique, because I didn't need to any deposition devices such as spin-coater, thermal evaporation devices, which are more expensive devices, to investigate the optical properties of the F8T2 polymer. This solution technique is more accurate than a film technique, because prior, during and after the coating of a film, various impurities may occur on the surface of the film and these disadvantages adversely affect the optical properties of the material. The maximum absorption wavelength (λ_{max}) of the solutions of the F8T2 for 1.200 and 0.800 µM was found to be 455 nm, while the λ_{max} of the F8T2 polymer for DCM, THF and Chloroform solvents were found to be 447, 453 and 455 nm, respectively. The yellow light of the F8T2 polymer is emitted 586 nm. The maximum mass extinction coefficient (α_{max}) value (64.763 $Lg^{-1}cm^{-1}$) of the

F8T2 polymer for DCM solvent is the highest value, while the α_{max} value (59.105 $Lg^{-1}cm^{-1}$) of the F8T2 polymer for Chloroform is the lowest value. The absorption band edge values of the solutions of the F8T2 polymer shift from 2.371 to 2.203 eV with increasing molarity. The direct energy-gap (E_{gd}) values (2.413 and 2.387 eV, respectively) of the F8T2 polymer for 0.800 μM and Chloroform solvent are the highest values, while the E_{gd} values (2.220 and 2.279 eV) of the F8T2 polymer for 19.737 μM and THF solvent are the lowest values. The indirect energy-gap (E_{gid}) values (2.345 and 2.305 eV, respectively) of the F8T2 polymer for 0.800 μM and Chloroform solvent are the highest values, while the E_{gid} values (2.113 and 2.053 eV) of the F8T2 polymer for 19.737 μM and THF solvent are the lowest values. The obtained E_{gid} values of the F8T2 polymer are more lower than that of the obtained E_{gd} values of the F8T2 polymer. The optical band-gap of the F8T2 polymer at different molarities can be found from the plots of $(\alpha h\nu)^2$ and $(\alpha h\nu)^{1/2}$ vs. E, the absorption band edge and the first decrease of transmittance spectra of the F8T2 polymer. The optical band-gap of the solution of the F8T2 polymer was decreased with increasing molarities and using THF solvent among DCM, THF and Chloroform solvents.

ACKNOWLEDGMENTS

This work was supported by The Management Unit of Scientific Research Projects of Muş Alparslan University (MUSBAP) under Project 0001. The author is grateful to Mrs. Hilal Gözler who is R&D Scientist and Nanomagnetic Instruments Co. because of helping with the AFM measurements.

REFERENCES

[1]. Briseno, A.L., Mannsfeld, S.C., Ling, M.M., Liu, S., Tseng, R.J., Reese, C., Roberts, M.E., Yang, Y., Wudl, F., Bao, Z., Patterning organic single-crystal transistor arrays, *Nature,* 444 (7121), 913-917, 2006.

[2]. Lim, J.A., Liu, F., Ferdous, S, Muthukumar, M., Briseno, A.L., Polymer semiconductor Crystals, *materialstoday*, 13(5), 14-24 2010.

[3]. de Boer, R.W.I., Gershenson, M.E., Morpurgo, A.F., Podzorov, V., Organic single-crystal field-effect transistors, *Phys. Status Solidi a-Appl. Res.,* 201 (6), 1302-1331, 2004.

[4]. Salleo, A., Charge transport in polymeric transistors, *materialstoday,* 10(3), 38-45, 2007.

[5]. Werzer, O., Matoy, M., Smilgies, D.M., Rothmann, M.M., Strohriegl, P., Resel, R., Uniaxially Aligned Poly[(9,9-dioctylfluorenyl-2,7-diyl)-cobithiophene] Thin Films Characterized by the X-ray Diffraction Pole Figure Technique, *Journal of Applied Polymer Science*, 107, 1817–1821,2008.

[6]. Kajii, H., Kasama, D., Ohmori, Y., Polymer Light-Emitting Diodes Fabricated Using Poly(9,9-dioctylfuorene) Gel by Thermal Printing Method, *Jpn. J. Appl.*

Phys., 47, 3152-3155, 2008.

[7]. Kajii, H., Koiwai, K., Hirose, Y., Ohmori, Y., Top-gate-type ambipolar organic field-effect transistors with indium–tin oxide drain/source electrodes using polyfluorene derivatives, 2010, *Organic Electronics,* 11, 509–513, 2010.

[8]. Asada, K., Kobayashi, T., Naito, H., Control of Effective Conjugation Length in Polyfluorene Thin Films, *Jpn. J. Appl. Phys.*, 45, L247-L249, 2006.

[9]. Sirringhaus, H., Wilson, R.J., Friend, R.H., Inbasekaran, M., Wu, W., Woo, E.P., Grell, M., Bradley, D.D.C., Mobility enhancement in conjugated polymer field-effect transistors through chain alignment in a liquid-crystalline phase, *Appl Phys Lett* ,77, 406-408, 2000.

[10]. Salleo, A., Street, R.A., Light-induced bias stress reversal in polyfluorene thin-film transistors, *J Appl Phys*., 94, 471-479, 2003.

[11]. Salleo, A., Chabinyc, M.L., Yang, M.S., Street, R.A., Polymer thin-film transistors with chemically modified dielectric interfaces, *Appl Phys Lett*, 81, 4383-4385, 2002.

[12]. Boucle, J., Ravirajan, P., Nelson, J., Hybrid polymer–metal oxide thin films for photovoltaic applications, *J. Mater. Chem.,* 17, 3141-3153, 2007.

[13]. Pattison, L.R., Hexemer, A., Kramer, E.J., Krishnan, S., Petroff, P.M., Fischer, D.A., Probing the ordering of semiconducting fluorene-thiophene copolymer surfaces on rubbed polyimide substrates by near-edge X-ray absorption fine structure, *Macromolecules*, 39, 2225-2231, 2006.

[14]. Jo, J., Vak, D., Noh, Y.Y., Kim, S.S., Lim, B., Kim, D.Y., Effect of photo- and thermo-oxidative degradation on the performance of hybrid photovoltaic cells with a fluorene-based copolymer and nanocrystalline TiO_2, *J. Mater. Chem.,* 18, 654-659, 2008.

[15]. Sirringhaus, H., Kawase, T., Friend, R.H., Shimoda, T., Inbasekaran, M., Wu, W., Woo, E.P., High-Resolution Inkjet Printing of All-Polymer Transistor Circuits, *Science,* 290, 2123-2126, 2000.

[16]. Huang, J.H., Yang, C.Y., Ho, Z.Y., Kekuda, D., Wu, M.C., Chien, F.C., Chen, P., Chu, C.W., Ho, K.C., Annealing effect of polymer bulk heterojunction solar cells based on polyfluorene and fullerene blend, *Organic Electronics*, 10, 27–33, 2009.

[17]. Gather, M.C., Bradley, D.D.C., An improved optical method for determining the order parameter in thin oriented molecular films and demonstration of a highly axial dipole moment for the lowest energy pi-pi* optical transition in poly(9,9-dioctylfluorene-co-bithiophene), *Adv. Funct. Mater*. 17(3), 479-485, 2007.

[18]. Lim, E., Jung, B.J., Chikamatsu, M., Azumi, R., Yoshida, Y., Yase, K., Do, L.M.,

Shim, H.K., Doping effect of solution-processed thin-film transistors based on polyfluorene, *J. Mater. Chem.*, 17, 1416-1420, 2007.

[19]. Heredia, A., Bui, C.C., Suter, U., Young, P., Schaffer, T.E., Elastic properties of myelinated and de-myelinated mouse peripheral axons by atomic force microscopy, *NeuroImage*,37, 1218-1226, 2007.

[20]. Kumar, B.R., Rao, T.S., AFM Studies on surface morphology, topography and texture of nanostructured zinc aluminum oxide thin films, *Digest Journal of Nanomaterials and Biostructures,* 7(4), 1881-1889, 2012.

[21]. Nesheva, D.D., Vateva, E., Levi, Z., Arsova, D., Thin film semiconductor nanomaterials and nanostructures prepared by physical vapour deposition: An atomic force microscopy study. J. Phys Chem Solids, 68, 675-680, 2007.

[22]. Marchetto, D., Rota, A., Calabri, L., Gazzadi, G.C., Menozzi, C., Valeri, S., AFM investigation of tribological properties of nano-patternedsiliconsurface, *Wear,* 265, 577-582, 2008.

[23]. Jalili, N., Laxminarayana, K., A review of atomic force microscopy imaging systems: application to molecular metrology and biological sciences, *Mechatronics*, 14, 907-945, 2004.

[24]. Kwoka, M., Ottaviano, L., Szuber, J., AFM study of the surface morphology of L-CVD SnO_2 thin films, *Thin Solid Films*, 515, 8328-8331, 2007.

[25]. Nagabhushana, K.R., Lakshminarasappa, B.N., Rao, K.N., Singh, F., Sulania, I., AFM and photoluminescence studies of swift heavy ion induced nanostructured aluminum oxide thin films. Nucl. Instr. & Meth. Phys. Res. B 266, 1049-1054, 2008.

[26]. Gizli, N., Morphological characterization of cellulose acetate based reverse osmosis membranes by Atomic Force Microscopy (FM) effect of evaporation time, *Chemistry & Chemical Technology*, 5(3), 327-331, 2011.

[27]. Noureddine, T., Polycarpou, A.A., Modeling the effect of skewness and kurtosis on the static friction coefficient of rough surfaces, *Tribology International,* 37, 491–505, 2004.

[28]. Goldys, E.M., Shi, J.J., Linear and Nonlinear Intersubband Optical Absorption in a Strained Double Barrier Quantum Well, *Phys. Status Solidi B*, 210, 237-248, 1998.

[29]. Ahn, D., Chuang, S.L., Calculation of linear and nonlinear intersubband optical absorption in a quantum well model with an applied electric field, *IEEE J. Quantum Electron*, 23, 2196-2204, 1987.

[30]. Baghramyan, H.M., Barseghyan, M.G., Kirakosyan, A.A., Restrepo, R.L., Duque, Linear andnonlinearopticalabsorptioncoefficientsinGaAs/Ga1xAlxAs concentric

double quantum rings: Effects of hydrostatic pressure and aluminum concentration, *Journal of Luminescence*, 134, 594-599, 2013.

[31]. Kazarinov, R.F., Suris, R.A., Possibility of the amplification of electromagnetic waves in a semiconductor with a superlattice, *Sov. Phys. Semicond.*, 5, 707-709, 1971.

[32]. Miller, D.A.B., Quantum-well optoelectronic switching devices, *Int. J. High Speed Electron. Syst*., 1, 19-46, 1990.

[33]. Hood, T.H., Multiple quantum well (MQW) waveguide modulators, *J. Lightwave Technol.,* 6, 743-757, 1988.

[34]. Ward, H.C., Chapter IV: Profile Characterization, Rough Surfaces (T.R. Thomas Ed., Longman, London, 1982).

[35]. D.J. Whitehouse, Handbook of Surface and Nanometrology, 2nd edition CRC press 2010.

[36]. Kolanek, K., Tallarida, M., Karavaev, K., Schmeisser, D., In situ studies of the atomic layer deposition of thin HfO2 dielectrics by ultra high vacuum atomic force microscope, *Thin Solid Films*, 518, 4688–4691, 2010.

[37]. Alley, R.L., Mai, P., Komvopoulos, K., Howe, R.T., Surface roughness modification of interfacial contacts in polysilicon microstructures. Proceedings of the Seventh International Conference on Solid-State Sensors and Actuators, Transducers'93, Yokohama, Japan, 7–10 June 1993. p. 288–291, 1993.

[38]. Liu, X., Chetwynd, G., Gardner, J.W., Surface characterization of electro-active thin polymeric film bearings, *International Journal of Machine Tools of Manufacturer*, 38(5–6), 669–675, 1998.

[39]. http://www.imagemet.com/index.php?id=35&main=products&sub=applications

[40]. Beer, A., Determination of the absorption of red light in colored liquids, *Ann. Phys.*, 86, 78-88, 1852.

[41]. Li, Y., Scales, N., Blankenship, R.E., Willows, R.D., Chen, M., Extinction coefficient for red-shifted chlorophylls: Chlorophyll d and chlorophyll f, *Biochimica et Biophysica Acta,* 1817, 1292-1298, 2012.

[42]. M. Fox, Optical Properties of Solids. Oxford Master Series in Condensed Matter Physics (Oxford University Press, Oxford, 2001).

[43]. Macedo, A.G., Silva, D.C., Yamamoto, N.A.D., Micaroni, L., Mello, R.M.Q, Roman, L.S., Bilayer and bulk heterojunction solar cells with functional poly(2,2-bithiophene) films electrochemically deposited from aqueous emulsion, *Synthetic Metals*, 170, 63–68, 2013.